ACS Chemical Neuroscience

Letter

pubs.acs.org/chemneuro

Substituted 5,6-(Dihydropyrido[3,4-*d*]pyrimidin-7(8*H*)-yl)-methanones as P2X7 Antagonists

Jeannie Ziff, Dale A. Rudolph, Brice Stenne, Tatiana Koudriakova, Brian Lord, Pascal Bonaventure, Timothy W. Lovenberg, Nicholas I. Carruthers, Anindya Bhattacharya, Michael A. Letavic, and Brock T. Shireman*

Janssen Research & Development L.L.C., 3210 Merryfield Row, San Diego, California 92121, United States

Supporting Information

ABSTRACT: We describe the synthesis of a novel class of brain penetrating P2X7 antagonists with high potency at both the rat and human P2X7 receptors. Disclosed herein are druglike molecules with demonstrated target engagement of the rat P2X7 receptors after an oral dose. Specifically, compound **20** occupied the P2X7 receptors >80% over the 6 h time course as measured by an ex vivo radioligand binding experiment. In a dose−response assay, this molecule has a plasma EC_{50} of 8 ng/mL. Overall, **20** has suitable druglike properties and pharmacokinetics in rat and dog. This molecule and others disclosed herein will serve as additional tools to elucidate the role of the P2X7 receptor in neuropsychiatric disorders.

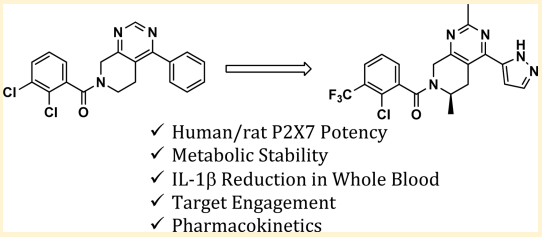

KEYWORDS: *P2X7, CNS, depression, IL-1β, 5,6-dihydropyrido[3,4-d]pyrimidin-7(8H)-yl) methanones, neuroinflammation*

First cloned in 1997, the P2X7 receptor (P2X7R) is a member of the purinergic ligand-gated ion channels that are expressed on microglia and astrocytes in the central nervous system (CNS).[1,2] Receptor activation by adenosine triphosphate (ATP) results in opening of the channel, ion flux, and the downstream release of cytokines such as IL-1β. Expression of P2X7 on immune cells has led to extensive research efforts by pharmaceutical companies, and academia focused predominantly on its role in the pathology of disease states related to peripheral inflammatory disorders.[3,4] Recent literature has established that P2X7 receptors in the CNS play a key role in modulating neuroinflammation via IL-1β release through the mechanism described above.[1,2] These findings were further corroborated by reports that IL-1β is involved in chronic stress models.[5,6] Furthermore, P2X7R antagonists have demonstrated efficacy in preclinical animal models of mood disorders.[7−12] While a variety of small molecule human specific, peripherally restricted P2X7 antagonists have been disclosed and entered clinical development, optimized molecules that specifically target receptors in the CNS and have acceptable rodent pharmacology are needed.[13,14] For example, GSK-1482160 (**1**) advanced to clinical trials for the potential treatment of neuropathic and inflammatory pain.[15,16] A potential drawback of **1**, that would preclude its use in preclinical animal models, is the reported speciation as indicated. Compound **1** possesses 100 times lower potency for the rat P2X7 receptor versus the human. Abbott has reported on the cyanoguanidine A-804598 (**2**), which was shown to be equipotent at human and rat P2X7 receptors.[17] However, significant occupancy of the P2X7 receptors in an ex vivo radioligand binding assay has only been reported following a subcutaneous dose.[18]

Based on the premise that a reduction of proinflammatory cytokines, such as IL-1β, in the CNS could be an effective treatment for neurophsychiatric disorders such as depression, we set out to discover a class of small molecule brain-penetrating P2X7 receptor antagonists. In addition to potency at human P2X7 receptors, a primary goal of our program was the discovery of molecules which also possessed good potency for the rat P2X7 receptors. This would allow for the eventual evaluation of advanced compounds in preclinical models.

We have previously reported the related piperazine compounds **3** and **4**.[11,18,19] The molecules were demonstrated to cross the blood-brain barrier and occupy the P2X7 receptors following a subcutaneous dose (sc) in an ex vivo radioligand binding experiment. In the case of **3** and **4**, sc dosing was required for extended occupancy. Our goals going forward included the discovery of a compound that engages the receptor after oral administration. An additional confounding pharmacology of **4** was its affinity for the serotonin reuptake transporter which would render any results from animal models difficult to interpret. In addition to the molecules illustrated above, we have recently reported the CNS penetrant P2X7 antagonists **5** and **6**.[20] Compound **5** demonstrated P2X7 target engagement after a 10 mg/kg oral dose and served as an advanced lead for further exploration. Compound **6** was shown to occupy the receptor in the same assay at 78% and 71% after a 10 mg/kg po dose at 0.5 and 2 h, respectively.

Special Issue: Neuroinflammation

Received: November 21, 2015
Accepted: January 12, 2016
Published: January 12, 2016

DOI: 10.1021/acschemneuro.5b00304
ACS Chem. Neurosci. 2016, 7, 498−504

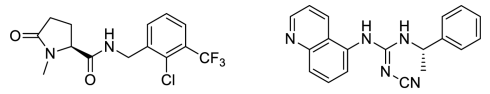

1
GSK 1482160
hP2X7 pIC_{50} = 8.5
rP2X7 pIC_{50} = 6.4

2
A-804598
hP2X7 pIC_{50} = 8.0
rP2X7 pIC_{50} = 7.7

Figure 1. P2X7 antagonists GSK 1482160 and A-804598.

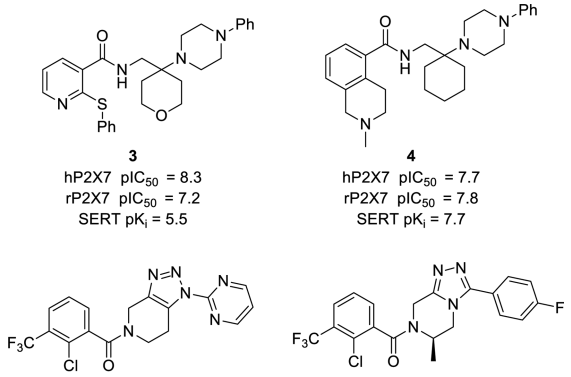

3
hP2X7 pIC_{50} = 8.3
rP2X7 pIC_{50} = 7.2
SERT pK_i = 5.5

4
hP2X7 pIC_{50} = 7.7
rP2X7 pIC_{50} = 7.8
SERT pK_i = 7.7

5
hP2X7 IC_{50} = 4.2 nM
rP2X7 IC_{50} = 6.8 nM
Metabolic Stability
ER (h/r): 0.61, 0.82

6
hP2X7 IC_{50} = 8.7 nM
rP2X7 IC_{50} = 14 nM

Figure 2. P2X7 antagonists from Janssen.

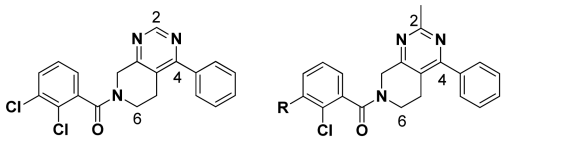

7
hP2X7 IC_{50} = 48 nM
rP2X7 IC_{50} = 4860 nM
Metabolic Stability
ER (h/r): 0.74, 0.94
cLogP=4.1

8, R=Cl
hP2X7 IC_{50} = 120 nM
rP2X7 IC_{50} = 4600 nM
Metabolic Stability
ER (h/r): <0.3, 0.76
cLogP=4.6

9, R=CF_3
hP2X7 IC_{50} = 240 nM
rP2X7 IC_{50} = 4790 nM
cLogP=4.8

Figure 3. Starting points 7–9.

In this Letter, we report our investigations into expansion of the 5-membered ring heterocycle to pyrimidine **7**, Figure 3. In addition to in vitro data and synthesis will include selected in vivo data for this series of molecules. Compound **7** possessed moderate potency in a Ca^{2+} mobilization assay, IC_{50} = 48 nM at the human P2X7 receptor and poor rat P2X7 potency (IC_{50} = 4860 nM).[21] Although **7** was shown to have a human extraction ratio (ER) of 0.74, addition of a methyl group in the 2 position of the pyrimidine resulted in compound **8** with improved stability in human microsomes (ER < 0.3). Even though this substitution resulted in a slight loss in human P2X7 potency, the substantial improvement in microsomal stability prompted a further investigation. Also illustrated in the figure is 2-chloro-3-trifluoromethyl benzamide **9**. Generally, these were used interchangeably for structure–activity relationship (SAR) purposes.

Our initial SAR began with a goal of lowering the cLog *P* by replacing the phenyl ring with a limited number of heterocycles as shown in Table 1. The *N*-2 substituted triazole **10** accomplished this goal while simultaneously improving potency at both the human and rat P2X7 receptors. Encouragingly, compound **10** also had an improved extraction ratio of <0.3

Table 1. Heterocycle Replacement at C-4

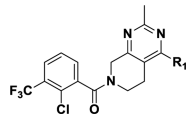

Compd	R1	IC_{50}[a,b] h/r (nM)[22]	hER[c]	cLogP
10		17.3/6.4	<0.3	3.2
11[d]		5011/ >10,000	n.t.	3.0
12		50/170	0.71	3.4
13		8.5/1140	<0.3	3.3
14		110/21	0.52	4.5
15		46/230	0.43	3.6

[a]In vitro human and rat P2X7 IC_{50} determined in a Ca^{2+} flux functional assay using a FLIPR instrument. [b]IC_{50}'s are the mean of at least three experiments in triplicate with a standard deviation less than 2-fold except where noted. [c]Extraction ratios are measured in a microsomal preparation. [d]Rat and human P2X7 IC_{50} from a single experiment in triplicate.

compared to the lead **7**. However, this compound was chemically unstable in solution under acidic conditions, limiting its progression. The isomeric *N*-1 isomer **11** gave a quite dramatic drop in P2X7 potency. The remaining heterocycles tested were C-linked. These included the thiazole **12**, pyrazole **13** and substituted pyrazoles **14** and **15**. Based on this data, the unsubstituted pyrazole **13** provided the best balance of human P2X7 potency (IC_{50} = 8.5 nM) and stability in human liver microsomes (ER < 0.3). However, the rat P2X7 potency still needed improvement (IC_{50} = 1140 nM). Moving forward, additional compounds were planned keeping the C-3 substituted pyrazole similar to **13** intact.

Further modifications to the 2-position of the pyrimidine demonstrated no real improvement in terms of human P2X7 potency as shown in Table 2. Replacement of the 2-position methyl group with a trifluoromethyl (**16**) resulted in an improvement in the rat potency, however not to a great extent. The cyclopropyl, amino, and dimethylamino (**17**–**19**) also offered no advantage to a methyl substituted analogue as shown. However, incorporation of a methyl group (**20**)[21] in the 6-position, alpha to the amide nitrogen, provided the needed improvement in rat P2X7 potency, IC_{50} = 10 nM, while maintaining human P2X7 potency, IC_{50} = 11 nM and a moderate extraction ratio (ER = 0.56). The C-2 ethyl (**21**) and isopropyl (**22**) analogues are shown in the table as well. When comparing all properties, neither compound provided a particular advantage over the methyl substituted analog.

DOI: 10.1021/acschemneuro.5b00304
ACS Chem. Neurosci. 2016, 7, 498–504

Table 2. Substitution at the 2 and 6 Positions

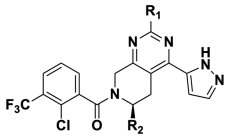

Compd	R_1	R_2	P2X7 IC_{50}[a,b] h/r (nM)[22]	hER[c]
16		H	64/240	<0.3
17		H	18/210	0.71
18		H	50/88	0.43
19		H	33/460	>0.95
20		Me	11/10	0.56
21[d]		Me	14/13	0.78
22[d]		Me	27/13	0.38

[a]In vitro human and rat P2X7 IC_{50} determined in a Ca^{2+} flux functional assay using a FLIPR instrument. [b]IC_{50}'s are the mean of at least three experiments in triplicate with a standard deviation less than 2-fold except where noted. [c]Extraction ratios are measured in a microsomal preparation. [d]Rat and human P2X7 IC_{50} from a single experiment in triplicate.

Based on these data, the decision was made to focus on 2-methylpyrimidines with an additional methyl group on the piperidine as illustrated for compound **20**. Not shown in the table is the CYP inhibition data for compound **20**, which in our CYP screening assay, was determined to be a moderate CYP3A4 inhibitor (IC_{50} of 3.3 μM).

Additional SAR was generated on the benzamide portion of the molecule as shown in Table 3. Various 2,3-disubstituted analogues were prepared to determine the effect on potency, ER and CYP 3A4 inhibition. The 2,3-dichloro analogue **24** was found to maintain potency and possessed improved microsomal stability relative to **20**. However, **24** was still a CYP inhibitor (3A4 IC_{50} = 1.9 μM). Substitutions with a 2-chloro-3-fluoro (**25**), 2-methyl-3-trifluoromethyl (**26**) or 2-fluoro-3-trifluoromethyl (**27**) did not provide any added benefit over **20** or **24**. Interestingly, the 2-chloro-4-fluoro and 2,4-difluoro analogues **28** and **29** gave a clean CYP profile and were stable in human liver microsomes (ER < 0.3). However, this intriguing result came at the expense of P2X7 potency. Potency could be restored with the 2-fluoro-4-chloro analogue **30** while maintaining a clean CYP profile and moderate stability in human liver microsomes (ER = 0.38). The 2,4-dichloro analogue **31** was made and found to be a CYP 3A4 inhibitor with otherwise good properties with regards to P2X7 potency and microsomal stability.

Based on the balance of human and rat P2X7 potency and human microsomal stability, compounds **20** and **30** were chosen for additional profiling.[23] Selected in vitro data for **20** and **30** are shown in Table 4. Compound **20** was found to have a high free fraction in human and rat. Additionally, brain tissue binding and permeability were deemed appropriate for a CNS compound. As indicated previously, stability in liver microsomes was considered moderate for **20** and CYP 3A4 inhibition

Table 3. Benzamide SAR

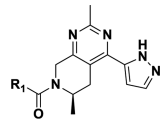

Compd	R_1	P2X7 IC_{50}[a,b] h/r (nM)[22]	hER[c]	CYP 3A4 IC_{50} (μM)
24		18/7.9	<0.3	1.9
25		53/220	<0.3	1.8
26		17/9.2	0.65	4.2
27		18/5.9	0.41	>10[d]
28		58/170	<0.3	>10
29		56/96	<0.3	>10
30		19/17	0.38	>10
31		11/14	<0.3	4.0

[a]In vitro human and rat P2X7 IC_{50} determined in a Ca^{2+} flux functional assay using a FLIPR instrument. [b]IC_{50}'s are the mean of at least three experiments in triplicate with a standard deviation less than 2-fold except where noted. [c]Extraction ratios are measured in a microsomal preparation. [d]2C9 IC_{50} = 3.4 μM

Table 4. In Vitro Data for 20 and 30

parameter	20	30
PPB h/r (% free)	6.5/5.6	21.6/15.2
BTB (% free)	3.2	7.4
CACO-2 B-A/B-A[a]	36.7/41.4	38.8/42.8
h/r (ER)[b]	0.56/0.58	0.38/0.41
P2X7 binding h/r K_i (nM)[c]	14.0/2.8	9.0/1.2
P2X7 whole blood assay IC_{50} (nM)[18d]	158	n.t.

[a]P_{app} reported in units of cm/s × 10^{-6}. [b]Extraction ratios are measured in a microsomal preparation. [c]K_i's are the mean of at least three experiments in triplicate with a standard deviation less than 2-fold. [d]Human whole blood IC_{50}'s are a result of 2 assay runs within 2-fold.

DOI: 10.1021/acschemneuro.5b00304
ACS Chem. Neurosci. 2016, 7, 498−504

Table 5. Rat Pharmacokinetics for 20 and 30

compd	%F (po)	CL[c]	C_{max}[d]	V_{ss}[e]
20[a]	115	26	768	1.7
30[b]	84	13.2	1100	1.6

[a]Compound was dosed as a solution in 20% HP-β-CD at 1.0 mg/kg iv and 5.0 mg/kg po (3 animals per dose). [b]Compound was dosed as a solution in 20% HP-β-CD with 2 equiv HCl at 1.0 mg/kg iv and 5.0 mg/kg po (3 animals per dose). [c]Clearance values are reported in mL/min/kg. [d]C_{max} is reported in ng/mL from the po arm. [e]V_{ss} is reported in L/kg.

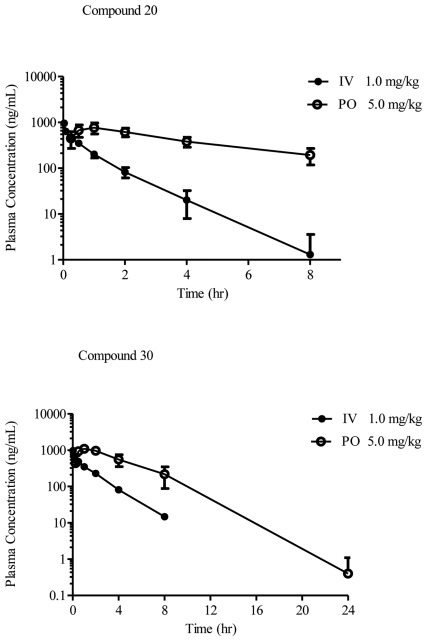

Figure 4. Rat IV and PO pharmacokinetics.

(IC_{50} = 3.3 μM) was viewed as a potential liability for **20.** Compound **30** had the benefit from an in vitro standpoint to have less risk for CYP 3A4 inhibition (IC_{50} > 10 μM), a higher free fraction in plasma and brain and increased stability in microsomes. Both compounds were potent in human and rat binding assays. Compound **20** was also evaluated in a whole blood assay to determine its inhibitory effects on the release of IL-1β. In this assay, **20** was determined to have an IC_{50} of 158 nM. Selectivity of compounds **20** and **30** was assessed by screening against a panel of 50 ion channels and GPCRs.

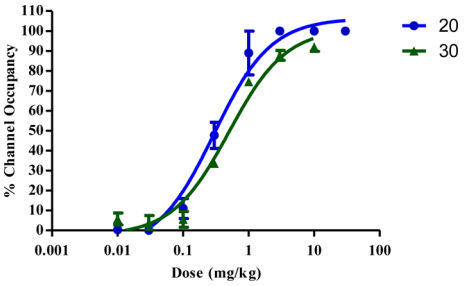

Figure 5. Ex vivo radioligand binding for **20** and **30**. Dose response study after oral administration. Ex vivo occupancy was measured after compound administration at 2 h for compound **20** and 1 h for compound **30**.

Table 7. Canine Pharmacokinetics for 20

compd[a]	%F	CL[b]	C_{max}[c]	V_{ss}[d]
20	35	8	571	2.3

[a]Compound was dosed as a solution in 20% HP-β-CD at 0.5 mg/kg iv and 2.5 mg/kg po (3 animals per dose). [b]Clearance values are reported in mL/min/kg. [c]C_{max} is reported in ng/mL from the po arm. [d]V_{ss} is reported in L/kg.

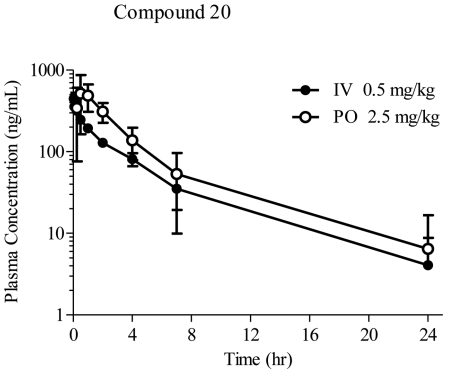

Figure 6. Canine IV and PO pharmacokinetics of **20**.

Neither of the compounds showed inhibition less than 50% at 1 μM against this panel. In addition, compound **30** was screened against the P2X1, P2X2, P2X3, P2X2/P2X3, and P2X4 ion channels and shown to have an inhibition less than 50% at 10 μM.

Encouraged by these results, we evaluated the compounds in rat pharmacokinetic experiments, Table 5 and Figure 4. Both

Table 6. Ex Vivo Radioligand Binding Experiments

time course % occupancy/brain/plasma (ng/mL) @ time point[a]	20[be]	30[cf]
0.5 h	81%	93%
	1877/4392	728/1860
2 h	93%	93%
	1639/3705	605/1641
6 h	83%	91%
	1427/4237	318/1089
dose response (po)[d]	**20**	**30**
ED_{50} (ng/mL)	0.3	0.5
B/P EC_{50}	5/8	22/101

[a]Reported level of P2X7 occupancy in rat brain with 2 animals per time point. [b]Compound **20** was dosed at 30 mg/kg po in the time course. [c]Compound **30** was dosed at 10 mg/kg po in the time course. [d]Reported occupancy in rat brain with 3 animals per time point. [e]P2X7 occupancy was measured at 2 h in the dose response assay. [f]P2X7 occupancy was measured at 1h in the dose response assay.

DOI: 10.1021/acschemneuro.5b00304
ACS Chem. Neurosci. 2016, 7, 498−504

compounds have good pharmacokinetics in rat following an oral dose. Gratifingly, the clearance was moderate and predicted by in vitro rat liver microsomes. Overall oral bioavailability and exposure were consistent with levels required to occupy the receptor at low dose assuming adequate penetration into the brain.

This was confirmed in the ex vivo radioligand binding assay[24] as shown below in Table 6 and Figure 5. Compound **20** occupied the receptor >80% over the complete time course (6 h) of the experiment after a 10 mg/kg po dose. This was comparable to compound **30** which demonstrated >90% occupancy. Subsequent to the time course experiment, we carried out a dose response with both compounds. In this ex vivo occupancy assay, compounds **20** and **30** have an ED_{50} of 0.3 and 0.5 mg/kg. These corresponded to plasma EC_{50}'s of 8 and 100 ng/mL for **20** and **30**, respectively.

Based on the plasma EC_{50} from the rat ex vivo radioligand binding experiment, **20** was progressed to a dog pharmacokinetic experiment as shown in Table 7 and Figure 6. Compound **20** was found to have moderate exposure (C_{max} = 571 ng/mL) after an oral dose as shown below, a low clearance (CL = 8 mL/min/kg) consistent with the measured extraction ratio (dog ER = 0.51), and an overall oral bioavailability of 35%. A human dose prediction resulted in an estimated dose of 100 mg bid in order to occupy the receptor 50% over 24 h.

METHODS

The route shown in Scheme 1 was utilized to obtain compounds **9**–**15**, **17**, and **19** by using the appropriately substituted amidine **33** at R_2 and Suzuki or Stille coupling partner. Beginning with the commercially available β-ketoester **32** and amidines **33**, pyrimidine formation utilizing K_2CO_3 in MeOH followed by chlorination with PPh_3 and CCl_4 in DCE gave the 4-chloropyrimidines **34**. Palladium catalyzed coupling with commercially available boronic acids or Stille reagents provided compounds **35**. Deprotection and amide bond formation using the acid chloride of 2-chloro-3-trifluoromethylbenzoic acid provided the desired products **9**–**15**, **17**, and **19**.

Compounds **16** and **18** were made according to the route shown in Scheme 2. Beginning with the appropriately substituted chloropyrimidine **36**, Suzuki coupling with the pyrazole boronic ester **37** provided the coupling product in 67–93% yield. Deprotection of the benzyl group using 1-chloroethylchloroformate and DIEA in DCM gave compounds **38**. Amide bond formation followed by removal of the THP group gave the desired molecules **16** and **18**.

Scheme 1. Synthesis of Compounds 9–15, 17, and 19[a]

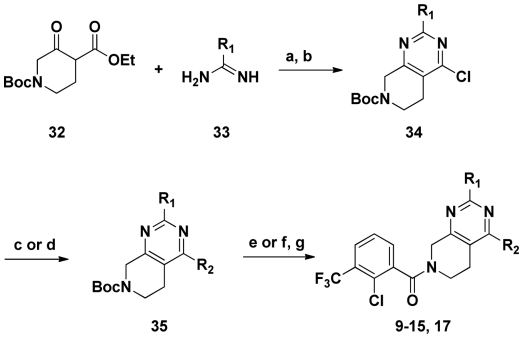

[a]Reagents and conditions: (a) K_2CO_3, MeOH, 70 °C; 92–99%; (b) PPh_3, CCl_4, DCE, 80 °C, 75–80%; (c) R_2BPin or $R_2B(OH)_2$, $Pd(PPh_3)_4$, 1 M Na_2CO_3 (aq), dioxane, 100 °C, 22–99%; (d) R_2SnBu_3, $Pd(PPh_3)_4$, dioxane, 140 °C, 15–99%; (e) TFA, DCM, quant.; (f) Et_3SiH, TFA, DCM, 85%; (g) 2-chloro-3-(trifluoromethyl)-benzoic acid, HATU, DIEA, DCM, 30–99%.

Scheme 2. Synthesis of Compounds 16 and 18[a]

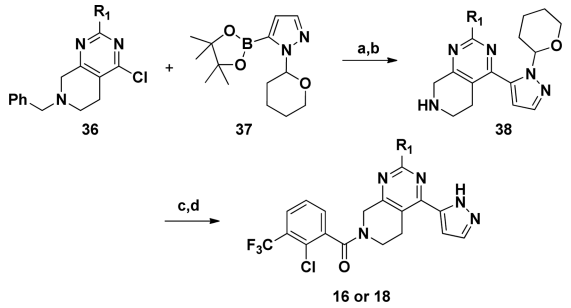

[a]Reagents and conditions: (a) $Pd(PPh_3)_4$, 1 M Na_2CO_3 (aq), dioxane, 100 °C, 67% (R1 = NH2), R2 = 93% (R1 = CF_3); (b) 1-chloroethyl chloroformate, DIEA, DCM, MeOH, 50 °C, quant.; (c) 2-chloro-3-(trifluoromethyl)benzoic acid, HATU, DIEA, DCM, 75% (R1 = NH2), 37% (R1 = CF_3); (d) Et_3SiH, TFA, DCM, 48% (R1 = NH2), 17% (R1 = CF_3).

Scheme 3. Synthesis of Compound 20 and Representative Synthesis for Compounds 21–31[a]

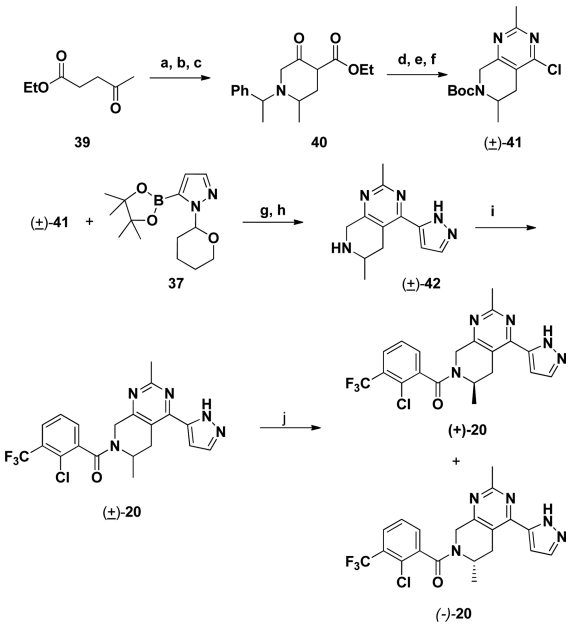

[a]Reagents and conditions: (a) (*R*/*S*)-α-methylbenzylamine, $NaBH(OAc)_3$, DCE, 90%; (b) ethyl glyoxylate, $NaBH(OAc)_3$; (c) DCE, >98%; KOtBu, $PhCH_3$, 63%; (d) 2-methylamidine hydrochloride, NaOEt, EtOH, 90 °C, 83%; (e) Boc_2O, ammonium formate, MeOH/THF, 10 wt % Pd/C, reflux, 82%; (f) PPh_3, CCl_4, DCE, 80 °C, 75%; (g) $Pd(PPh_3)_4$, 1 M Na_2CO_3 (aq), dioxane, 100 °C, 90%; (h) Et_3SiH, TFA, DCM, quantitative; (i) 2-chloro-3-trifluoromethylbenzoic acid, HATU, DIEA, DCM, 53%; (j) SFC resolution, 48% recovery for (+)-**20**.

Shown in Scheme 3 is the synthesis of compound **20**. Beginning with ester **39**, β-ketoester formation using the three-step sequence indicated provided compound **40** as a racemic mixture of diastereomers. Similar to what was described above, heterocycle formation using 2-methylamidine hydrochloride provided the intermediate pyrimidine. In this case, the benzyl group was replaced by a Boc protecting group using Pd/C and ammonium formate in the presence of Boc_2O. Chlorination of the Boc protected compound using PPh_3 and CCl_4 gave the 4-chloropyrimidine **41**. Suzuki cross-coupling with the boronate ester **37** gave the desired protected pyrazole in 75% yield. Simultaneous deprotection of the THP and Boc group gave the free amine followed by amide bond formation with 2-

DOI: 10.1021/acschemneuro.5b00304
ACS Chem. Neurosci. 2016, 7, 498–504

chloro-3-trifluoromethylbenzoic acid using HATU and DIEA in DCM gave the racemic compound (*R*/*S*)-**20** in 53% yield. Resolution to the individual enantiomers was carried out using SFC chromatography providing (+)-**20** and (−)-**20** in 48% and 49% yield, respectively. An analogous route was followed for compounds **21**-**31**.

In conclusion, we have reported a series of brain penetrating P2X7 antagonists with good potency at both the rat and human P2X7 receptors with excellent drug like properties. Compound **20** was shown to be effective in reducing IL-1β in an in vitro whole blood assay. The compounds exhibit good oral exposure in rat and dog which leads to extended receptor occupancy and a moderate human dose prediction of 100 mg BID. Although this class of molecules did display some liabilities with regard to CYP 3A4 inhibition, these improved compounds will prove useful as additional tool molecules to delineate the role of P2X7 antagonism in neuropsychiatric disorders. Further details will be reported in due course.

■ ASSOCIATED CONTENT

Supporting Information

The Supporting Information is available free of charge on the ACS Publications website at DOI: 10.1021/acschemneuro.5b00304.

Assay descriptions, synthetic procedures, and compound characterization (PDF)

■ AUTHOR INFORMATION

Corresponding Author

*E-mail: bshirema@its.jnj.com.

Author Contributions

J.Z., D.A.R., B.S., N.I.C., M.A.L., and B.T.S. contributed to the design and/or synthesis of the compounds in this manuscript. B.L. and P.B. were responsible for the ex vivo radioligand binding assay. A.B. and T.W.L were responsible for the in vivo and in vitro pharmacology. T.K. was responsible for the ADME and pharmacokinetic experiments.

Notes

The authors declare no competing financial interest.

■ ACKNOWLEDGMENTS

We thank Heather McAllister and David Speybrouck for analytical support.

■ REFERENCES

(1) Sperlagh, B., and Illes, P. (2014) P2X7 receptor: an emerging target in central nervous system diseases. *Trends Pharmacol. Sci. 35*, 537−547.

(2) Stokes, L., Spencer, S. J., and Jenkins, T. A. (2015) Understanding the role of P2X7 in affective disorders-are glial cells the major players? *Front. Cell. Neurosci. 9*, 258.

(3) Bartlett, R., Stokes, L., and Sluyter, R. (2014) The P2X7 Receptor Channel: Recent Developments and the Use of P2X7 Antagonists in Models of Disease. *Pharmacol. Rev. 66*, 638−675.

(4) Di Virgilio, F. (2015) P2X Receptors and Inflammation. *Curr. Med. Chem. 22*, 866−877.

(5) Goshen, I., Kreisel, T., Ben-Menachem-Zidon, O., Licht, T., Weidenfeld, J., Ben-Hur, T., and Yirmiya, R. (2008) Brain interleukin-1 mediates chronic stress-induced depression in mice via adrenocortical activation and hippocampal neurogenesis suppression. *Mol. Psychiatry 13*, 717−728.

(6) Zhang, Y., Liu, L., Liu, Y. Z., Shen, X. L., Wu, T. Y., Zhang, T., Wang, W., Wang, Y. X., and Jiang, C. L. (2015) NLRP3 Inflammasome Mediates Chronic Mild Stress-Induced Depression in Mice via Neuroinflammation. *Int. J. Neuropsychopharmacol. 18*, 1−8.

(7) Ortiz, R., Ulrich, H., Zarate, C. A., Jr., and Machado-Vieira, R. (2015) Purinergic system dysfunction in mood disorders: a key target for developing improved therapeutics. *Prog. Neuro-Psychopharmacol. Biol. Psychiatry 57*, 117−131.

(8) Wilkinson, S. M., Gunosewoyo, H., Barron, M. L., Boucher, A., McDonnell, M., Turner, P., Morrison, D. E., Bennett, M. R., McGregor, I. S., Rendina, L. M., and Kassiou, M. (2014) The first CNS-active carborane: A novel P2X7 receptor antagonist with antidepressant activity. *ACS Chem. Neurosci. 5*, 335−339.

(9) Csolle, C., Ando, R. D., Kittel, A., Goloncser, F., Baranyi, M., Soproni, K., Zelena, D., Haller, J., Nemeth, T., Mocsai, A., and Sperlagh, B. (2013) The absence of P2X7 receptors (P2rx7) on non-haematopoietic cells leads to selective alteration in mood-related behaviour with dysregulated gene expression and stress reactivity in mice. *Int. J. Neuropsychopharmacol. 16*, 213−233.

(10) Csolle, C., Baranyi, M., Zsilla, G., Kittel, A., Goloncser, F., Illes, P., Papp, E., Vizi, E. S., and Sperlagh, B. (2013) Neurochemical Changes in the Mouse Hippocampus Underlying the Antidepressant Effect of Genetic Deletion of P2X7 Receptors. *PLoS One 8*, e66547.

(11) Lord, B., de Haes, P., Drinkenburg, W., Bouwknecht, A., Ceusters, M., Bonaventure, P., Letavic, M., and Lovenberg, T. (2014) Pharmacology of a Novel Central Nervous System−Penetrant P2X7 Antagonist JNJ-42253432. *J. Pharmacol. Exp. Ther. 351*, 628−641.

(12) Wilkinson, S. M., Gunosewoyo, H., Barron, M. L., Boucher, A., McDonnell, M., Turner, P., Morrison, D. E., Bennett, M. R., McGregor, I. S., Rendina, L. M., and Kassiou, M. (2014) *ACS Chem. Neurosci. 5*, 335−339.

(13) For a recent review, see: Chrovian, C. C., Rech, J. C., Bhattacharya, A., and Letavic, M. A. (2014) P2X7 Antagonists as Potential Therapeutic Agents for the Treatment of CNS Disorders. *Prog. Med. Chem. 53*, 65−100.

(14) Guile, S. D., Alcaraz, L., Birkinshaw, T. N., Bowers, K. C., Ebden, M. R., Furber, M. R., and Stocks, M. J. (2009) Antagonists of the P2X7 Receptor. From Lead Identification to Drug Development. *J. Med. Chem. 52*, 3123−3141.

(15) Abdi, M. H., Beswick, P. J., Billinton, A., Chambers, L. J., Charlton, A., Collins, S. D., Collis, K. L., Dean, D. K., Fonfria, E., Gleave, R. J., Lejeune, C. L., Livermore, D. G., Medhurst, S. J., Michel, A. D., Moses, A. P., Page, L., Patel, S., Roman, S. A., Senger, S., Slingsby, B., Steadman, J. G. A., Stevens, A. J., and Walter, D. S. (2010) Discovery and Structure-Activity Relationship of a Series of Pyroglutamic Acid Amide Antagonists of the P2X7 Receptor. *Bioorg. Med. Chem. Lett. 20*, 5080−5084.

(16) Abberley, L., Bebius, A., Beswick, P. J., Billington, A., Collis, K. L., Dean, D. K., Fonfria, E., Gleave, R. J., Medhurst, S. J., Michel, A. D., Moses, A. P., Patel, S., Roman, S. A., Scoccitti, T., Smith, B., Steadman, J. G. A., and Walter, D. S. (2010) Identification of 2-oxo-N-(phenylmethyl)-4-imidazolidinecarboxamide Antagonists of the P2X7 Receptors. *Bioorg. Med. Chem. Lett. 20*, 6370−6374.

(17) Donnelly-Roberts, D. L., Namovic, M. T., Surber, B., Vaidyanathan, S. X., Perez-Medrano, A., Wang, Y., Carroll, W. A., and Jarvis, M. F. (2009) [^{3}H]A-804598 ([^{3}H]2-cyano-1-[(1S)-1-phenylethyl]-3-quinolin-5-ylguanidine) is a Novel, Potent, and Selective Antagonist Radioligand for P2X7 Receptors. *Neuropharmacology 56*, 223−229.

(18) Bhattacharya, A., Wang, Q., Ao, H., Shoblock, J. R., Lord, B., Aluisio, L., Fraser, I., Nepomuceno, D., Neff, R. A., Welty, N., Lovenberg, T. W., Bonaventure, P., Wickenden, A. D., and Letavic, M. L. (2013) Pharmacological Characterization of a Novel Centrally Permeable P2X7 Receptor Antagonist: JNJ-47965567. *Br. J. Pharmacol. 170*, 624−640.

(19) Letavic, M. A., Lord, B., Bischoff, F., Hawryluk, N. A., Pieters, S., Rech, J. C., Sales, Z., Velter, A. I., Ao, H., Bonaventure, P., Contreras, V., Jiang, X., Morton, K. L., Scott, B., Wang, Q., Wickenden, A. D., Carruthers, N. I., and Bhattacharya, A. (2013) Synthesis and Pharmacological Characterization of Two Novel, Brain Penetrating P2X7 Antagonists. *ACS Med. Chem. Lett. 4*, 419−422.

(20) Savall, B. M., Wu, D., De Angelis, M., Carruthers, N. I., Ao, H., Wang, Q., Lord, B., Bhattacharya, A., and Letavic, M. A. (2015) Synthesis, SAR, and Pharmacological Characterization of Brain Penetrating P2X7 Antagonists. *ACS Med. Chem. Lett. 6*, 671−676.

DOI: 10.1021/acschemneuro.5b00304
ACS Chem. Neurosci. 2016, 7, 498−504

(21) Rudolph, D. A., Alcazar, J., Ameriks, M. K., Anton, A. B., Ao, H., Bonaventure, P., Carruthers, N. I., Chrovian, C. C., De Angelis, M., Lord, B., Rech, J. C., Wang, Q., Bhattacharya, A., Andres, J. I., and Letavic, M. L. (2015) *Bioorg. Med. Chem. Lett. 25*, 3157−3163.
(22) Compounds were screened at 10 μM in a human peripheral blood monocyte (HPBMC) assay prior to determination of IC_{50}'s to test for P2X7 antagonism. The description of these and other biological assays can be found in refs 18−19.
(23) Absolute stereochemistry was determined by analogy to ref 21.
(24) For a description of the ex vivo radioligand binding assay, see: Lord, B., Ameriks, M. K., Wang, Q., Fourgeaud, L., Vliegen, M., Verluyten, W., Haspeslagh, P., Carruthers, N. I., Lovenberg, T. L., Bonaventure, P., Letavic, M. A., and Bhattacharya, A. (2015) A Novel Radioligand for the ATP-gated Ion Channel P2X7: [3H] JNJ-54232334. *Eur. J. Pharmacol. 765*, 551.

DOI: 10.1021/acschemneuro.5b00304
ACS Chem. Neurosci. 2016, 7, 498−504